Paper No.
04456

CORROSION 2004

SURFACE AREA DEPENDENCE OF ELECTROCHEMICAL POTENTIAL NOISE OF ALUMINUM ALLOYS IN CHLORIDE MEDIA

Idelfonso Arrieta*, Alberto Sagüés**, Babu Joseph*
*Department of Chemical Engineering
**Department of Civil and Environmental Engineering
University of South Florida
4202 East Fowler Ave. Tampa, FL 33620

ABSTRACT

The magnitude of electrochemical potential noise of aluminum alloys 1100, 2024 and 5052 in naturally aerated chloride solutions decreased approximately with increasing square root of specimen surface area in contact with the electrolyte. The experimental behavior was consistent with the predictions of a simplified model that assumed random generation of similar independent anodic events at a rate proportional only to the specimen area. The potential fluctuation from each individual event decreased with increasing specimen area due to the corresponding increase in interfacial admittance. This factor, coupled with statistical addition of the contribution of individual events, resulted in a model output reproducing the observed inverse square root dependence on area. The model applicability was demonstrated by nearly replicating experimental behavior when using as input interfacial polarization parameters that were obtained from independent electrochemical impedance and potentiodynamic tests.

Keywords: Electrochemical Noise, Surface Area Dependence, Aluminum, Chloride, Modeling, Impedance, Capacitance.

INTRODUCTION

Electrochemical potential noise under open circuit potential (OCP) conditions (abbreviated as EN hereafter) often reflects episodes where a predominantly anodic dissolution stage is followed by a predominantly cathodic recovery period. The episodes may be seen taking place individually, or as superimposed events if they happen frequently enough. In the case of EN due to metastable pitting in Al alloys[1,2], the anodic event covers the period from pit birth to death, and can be short-lived (e.g. ~1 second). Because of polarization of the cathodic reaction, much of the electronic charge left in the metal during such fast anodic stage is stored in the interfacial capacitance (Figure 1). A downward potential step of size

V=Q/C results, where Q is the Faradaic charge equivalent of the metal oxidized in the pit, and $C=C_{dl}.A_S$ is the total interfacial capacitance, with C_{dl}=specific interfacial capacitance and A_S= surface area of the metal-electrolyte interface. Upon termination of the anodic event, the cathodic reaction consumes the stored charge relatively slowly, eventually returning to the OCP value that existed before the anodic event unless another pitting event starts in the interim.

The amplitude of the EN signal in this type of transient is dominated by the height of the potential step during the anodic stage. For a given typical value of charge per event, step height would be expected to decrease with increasing A_S if the scenario discussed above applies. Such decrease has been reported[3-6] but it has received relatively little attention in the literature. This effect is important as adequate signal amplitude is necessary for the practical application of EN as a corrosion monitoring technique. Thus, this investigation sought to further elucidate the effect of specimen surface area on amplitude by a combination of experiments and modeling.

For the present work we used Al alloys in naturally aerated neutral chloride media, where EN signals tend to be strong and amenable to straightforward characterization.[7-10] EN signals were analyzed primarily in the time domain, and correlated with information on interfacial capacitance and cathodic kinetics obtained from transient and quasi-static polarization measurements. The EN amplitude-surface area trends obtained were examined with a quantitative model based on the scenario described above.

EXPERIMENTAL PROCEDURE

Aluminum alloys 1100, 2024 and 5052 (Table 1, including UNS designations) were used, representative of commercially pure metal, a precipitation hardening alloy and a solid solution hardening alloy respectively. The materials were obtained as strip coupons from Metal Samples, Inc.[(1)] Portions of the coupons were cut out, embedded in metallographic epoxide cylinders and wet-ground to a 600 grit finish to expose flat portions with surface area of ~0.02 cm^2, or ~0.2 cm^2 or ~4 cm^2. Contact to the exterior was made by an otherwise isolated copper wire that was attached to the back of the aluminum alloy specimen in the embedded region.

The specimens were placed in a test cell with the exposed metal surface in a vertical plane. The test cell included typically three specimens in a beaker containing ~ 300 cm^3 of distilled water to which 3.5% NaCl was added. A Saturated Calomel Electrode (SCE) was placed in the center of the beaker. The test cell was placed inside a grounded Faraday's cage. The difference of potential between the specimen and the SCE was measured with a data acquisition system (DAS) having a high input impedance (~ 2 G ohm) and low bias current (<50 nA) front end, 12-bit resolution and a data acquisition rate of 10/sec. A dc voltage compensator (VC) was placed in series with the DAS input and adjusted to obtain a starting compensated potential close to the zero of the recording window at the beginning of each EN record. Depending on the noise amplitude, the recording window was either 20 mV or 200 mV wide. EN records were 300 s long. The potential value indicated by the VC was designated as the nominal OCP value for the EN record. EN records were collected starting shortly after specimen immersion and obtained periodically typically over a one day period.

---

(1) Metal Samples Inc., 152 Metal Samples Rd., Munford, AL, USA, 36268

The same test cell but with one specimen at a time and with the addition of a high-density graphite counter electrode was used for Electrochemical Impedance Spectroscopy (EIS) measurements at the OCP in the frequency range 0.01-300 Hz, with a sinusoidal potential perturbation of 10 mV rms. Cathodic potentiodynamic (PD) scans starting and ending at the OCP, at a scan rate of ~ 0.167 mV/s, were also conducted. A CMS 300 system[2] was used for both techniques. All EIS and PD tests were conducted in naturally aerated distilled water; as explained later this medium permitted obtaining information on cathodic polarization parameters while minimizing obscuring random anodic events.

All tests were performed in duplicate. Results shown are typical unless otherwise indicated.

RESULTS AND DISCUSSION

The EN measurements showed a large number of events for all three alloys and all exposed surface area sizes during the first several hours after immersion. Figures 2-4 are typical of that period. Events became less frequent afterwards as illustrated in Fig. 5. Individual noise events, whenever identifiable, tended to follow the pattern shown in Figure 1 in the Introduction. The magnitude of the noise events was large for the smallest surface area specimens and decreased with increasing surface area. The EN magnitude was quantified by descriptors in the time domain by computing the potential standard deviation σ_E and range R, for several 300 s records collected during the first few hours of immersion:

$$s_E = \sqrt{\frac{\sum (E_i - E_{av})^2}{n_d - 1}} \qquad (1)$$

where n_d is the number of potential data in the record (3,000), E_i is the potential measured at time step i, E_{av} is the average potential, and

$$R = E_{max} - E_{min} \qquad (2)$$

where E_{max} and E_{min} are the maximum and minimum potential values in each record respectively.

Results of these calculations are shown in Figures 6-8. There is a general power-law decrease in EN magnitude, as measured by either descriptor, with increasing surface area. The power exponent is ~ -0.4 to -0.5 for all three aluminum alloys.

Power spectrum density (PSD) analysis of the EN records revealed high-frequencies roll-off slopes ranging from 23 db/decade to 26 db/decade during the early immersion times that correspond to the data in Figures 2-8. The roll-off slopes were essentially independent of specimen surface area.

The average OCP during the first several hours following immersion was ~-750 mV for alloys 1100 and 5052, and ~-625 mV for alloy 2024. The surface of alloys 1100 and 5052

[2] CMS 300 is a trade name of Gamry Instruments, 734 Louis Drive Warminster, PA, USA, 18974

remained bright and showed no macroscopic evidence of corrosion (per visual examination with a low magnification lens) during the first two days of immersion. Alloy 2024 showed discoloration and white spots associated with stable pits after about 6 hours of immersion. All three alloys showed macroscopic evidence of crevice corrosion around the perimeter typically after 2 days immersion.

The cathodic PD tests (all in distilled water) yielded polarization curves as those exemplified in Figure 9 for alloy 5052. The results are corrected for solution resistance. An average of the forward and return currents was calculated for each potential (also exemplified in Fig. 9) and converted into current density by division over the specimen area. The cathodic current density i_c and slope of the potential vs. log current density curve were evaluated for each alloy at the typical value of OCP observed in the NaCl solution tests. From those values an effective cathodic polarization slope β_c and an effective cathodic polarization resistance $R_p = \beta_c/2.3\, i_c$ [11] were obtained for each alloy and listed in Table 2.

It is noted that the PD tests were conducted in distilled water to minimize the presence of transient anodic events so as to characterize the polarization of the cathodic reaction only. The background passive anodic dissolution current density was assumed to be negligible. The rate of the cathodic reaction (likely to be oxygen reduction under neutral conditions, generally as $O_2 + 2\, H_2O + 4e^-$? $4\, OH^-$), was assumed to depend approximately only on potential and not be affected greatly by the chloride content or by anodic events, except for their role in establishing a mixed OCP value upon chloride contamination. The parameter β_c is not construed to be a Tafel slope, but is rather treated as an empirical polarization slope that may include a concentration polarization component and other possible kinetic complications.

The EIS tests (all in distilled water, and at the distilled water OCP) gave results for alloys 1100 and 5052 as those exemplified for alloy 5052 in Fig. 10. After subtracting the solution resistance, the simple depressed semicircle appearance was interpreted as resulting from the parallel combination of an ohmic admittance due to the Faradaic process operating at the mixed distilled-water OCP, and a non-ideal interfacial capacitance acting as a constant phase-angle element (CPE) of admittance $Y_{CPE}=Y_0\ (j\omega)^n$ [11,12]. The EIS data were processed accordingly with the model editor built-in the EIS instrumentation system to obtain the values of Y_0 and n for each alloy, which are listed in Table 2. Alloy 2024 showed a high frequency semicircle comparable to those in the other alloys, but also an additional semicircle at lower frequencies. This behavior was modeled as a series combination of two parallel ohmic admittance-CPE combination subcircuits. Table 2 lists for alloy 2024 only the parameters for the CPE in the subcircuit corresponding to the semicircle observed at the highest frequencies.

The EIS tests were conducted in distilled water to preserve causality (otherwise compromised by anodic transients) in the impedance response.[13] It was assumed that the surface-averaged interfacial capacitance was not strongly dependent on potential, chloride concentration, or the presence of small localized corrosion spots, so that the values obtained in distilled water would be approximately applicable to the mixed system under chloride contamination. Other than being used in the EIS spectrum fit to calculate capacitance parameters, the Faradaic admittance at the distilled-water OCP is not relevant to the chloride contaminated system and was dropped from further consideration.

MODELING

EN Trends

The EN patterns observed in these systems resemble a superposition of events like those shown in Figure 1. This behavior is typical of metastable pitting in Al alloys, as is the PSD signature observed.[3] The decay in event frequency after several hours of exposure suggests that some depletion of metastable pit nucleation sites[7] took place as time progressed. However, some of the signal may also derive from electrochemical fluctuations in stable pits (especially in alloy 2024) and from the onset of crevice corrosion in all three alloys during the later stages of exposure.

Regardless of the source of EN, the results clearly document a decrease of EN magnitude with increasing specimen surface area. This trend follows the hypothesis indicated in the Introduction that total interfacial capacitance, increasing with specimen area, lowers the step height of the portion of the event corresponding to the active stage and consequently lowers the magnitude of the EN. However, the overall effect of increasing area is complicated by the behavior during the decay portion of individual events, and by the superposition of multiple events. To quantitatively assess this behavior, a simplified EN simulation model was prepared following Cottis et al.[14,15] but allowing for polarization resistance of the cathodic reaction.

Model Formulation

The model considered the observed amplitude of individual noise events, and electrochemical reaction parameters at the metal-electrolyte interface as determined from the PD and EIS experiments. It was assumed that at the surface of the specimen random anodic events occur at a given average rate per unit time and unit area and, for simplicity, that each anodic event left always the same amount of negative charge in the metal. The anodic event was considered to be very short so that the charge consumed by cathodic reactions during the anodic stage was negligible. Thus the anodic stage causes the potential to decrease by the ratio of the anodic charge to the capacitance of the metal-electrolyte interface. The charge was consumed after the anodic stage by the cathodic reaction, with a time constant equal to the product of the polarization resistance of the cathodic reaction (which is the only reaction considered for the cathodic stage) and the total interfacial capacitance, both corrected to reflect the specimen surface area. However, the area corrections cancel each other and consequently the time constant and the shape of the transients become area-independent. Implicit in this treatment is the assumption that the potential fluctuations were small enough to use a linear polarization approximation for the cathodic reaction near the OCP. The effects of separate events on the potential were considered to be independent and additive. The model integrated these effects over a simulated sampling period where a given total number of calculated data points are produced for uniform time steps.

The model inputs were:

1. Number of data points (n_s).
2. Data acquisition step (Sampling time) (T_s).
3. Surface area (A_s) of the specimens.
4. Rate of events (n_e).

5. Effective Interfacial Capacitance of the metal-electrolyte interface (C_{eff}).
6. Charge (q_{ev}) released per event.
7. Polarization resistance (R_p) of the cathodic reaction.

From the input variables, the following parameters were calculated:

1. Duration of the test, $T_d = n_s.T_s$
2. Number of events, $N_{ev} = n_e.T_d.A_s$
3. Potential step height of each event, $h_{ev} = q_{ev} / C_{eff}.A_s$
4. Time constant of the cathodic stage, $\tau = C_{eff}.R_p$

The model generated the following:

1. Random numbers (r_k) which assigned the moment at which each of the N_{ev} events happened.

2. The individual potential waveform (h) after each event as:

$$h_{k,i} = h_{ev}.e^{\left[\frac{-(i-r_k).T_s}{t}\right]}.f_m \qquad (3)$$

where i is the simulated data index and k=1,2,…,N_{ev}. A multiplying factor (f_m)=0 for ($i-r_k$) < 0 and 1 otherwise, was introduced to limit the event response to the time following the event.

3. The cumulative EN output H of all the events was obtained by the sum of the individual potential contributions:

$$H_i = \sum_{k=1}^{N_{ev}} h_{k,i} \qquad (4)$$

The model was implemented for a system representative of the average behavior of the three alloys. Input parameters values are listed in Table 3. Timing parameters n_s and dt reflect the 300 s record length and the data acquisition rate used. A_s values represented the three specimen dimensions used. The assigned value of n_e (and calculated N_{ev}) was based on the typical rate of events observed in the EN records of the smallest surface area specimens, where individual events were more easily identified.

The polarization resistance value adopted for the model calculation was 130 kΩ cm^2, which was the approximate average of the values listed in Table 2 for all three alloys. As shown also in Table 2, interfacial capacitance in all three alloys was non-ideal and followed approximately CPE behavior. The average CPE parameters for all three alloys are n~0.67 and Y_0~13.2 μF s^n / cm^2. Following previous analysis[12] of the time domain response of a CPE a value of C_{eff} = 20 μF/cm^2 was adopted, which yields a C_{eff} R_p time constant τ in the order of the characteristic time of a parallel CPE – R_p combination with the above values. Note that value of τ (2.6 s) is in the order of the decay times apparent for typical single events in Figures

2-4. The value of C_{eff} is also in the general range of commonly reported capacitance values for finely ground Al alloy surfaces in aqueous media.[16,17]

Individual event records in Figures 2-5 (best seen with the smallest surface area A_S~0.04 cm^2) show that h_{ev} in the specimens was in the order of 25 mV. A nominal value of $q_{ev} = h_{ev} C_{eff} A_S = 2\ 10^{-8}$ C then results. For the model description however, it was chosen to use q_{ev} as the input variable and h_e as a derived magnitude. It is noted that if anodic dissolution occurred as Al ? $Al^{+3} + 3e^-$, the value of q_{ev} would correspond to the formation of an ideal hemispherical pit diameter of ~ 1 μm. Such small estimated size is consistent with the observed featureless appearance of the specimen surfaces at low magnifications during the early stages of exposure, and also in agreement with other reports of metastable pitting morphology in Al alloys.[10]

Results and Significance

The simulated time records and the corresponding trends are shown in Figures 11-12. While the assumption of a flat q_{ev} value caused some crude discretization at the smallest A_S, the modeled shape and magnitude of the time records generally resemble actual behavior. Also as in the actual case, the amplitude of the simulated fluctuations at OCP decreased with increasing A_S. The s and R values were calculated disregarding the first 10% of the simulated test interval to better reflect a steady state pattern. The s and R trendlines and associated parameters s_0 and R_0 and n_s and n_R , listed in Figure 12, were also quite similar to those from experiment. PSD analysis of the modeled EN response yielded roll-off slopes of ~18 db/decade, somewhat smaller but still comparable to those observed experimentally. The modeled roll-off slope also approaches the value of 20 db/decade predicted by Bertocci et al[18] for potential transients that start abruptly.

The modeled and actual response are consistent with the expectation, indicated in the introduction, that the increase in surface area would lower h_{ev} and thus the EN magnitude. However, both the experimental and modeled trends indicated that the EN magnitude (as measured by either σ or R) decreased with a ~1/2 power of A_S while the value of h_{ev} in the model varies proportional to A_S^{-1}. This apparent inconsistency is resolved semiquantitatively by recalling that under the model assumptions an increase in area is also accompanied by an increase in the number of events per unit time, $n_e A_S$, which lessens the effect of reduced h_{ev} on σ. From the form of Eq. (1) and for events of the same shape and size, σ would be expected to increase proportional to the square root of the number of events. The range R would be anticipated to generally follow the σ trend by analogy with the case of a normal distribution[19]. These expectations were tested with a series of model calculations where A_S was kept constant while n_{ev} varied, which confirmed that in such case σ and R were both approximately proportional to $n_e^{1/2}$ (also when only q_{ev} was varied the computed EN level was simply proportional to the first power of h_{ev}). Consequently, as A_S increases the effect of a greater rate of events should be proportional to $A_S^{1/2}$ for a combined proportionality to $A_S^{-1}A_S^{1/2}$ ~ $A_S^{-1/2}$ as observed. It is noted that increasing area elevates the total Faradaic component as well as the total capacitive component of the interfacial admittance, so a similar area effect should apply also for localized transients of arbitrary shape as shown in a more general predictive treatment by Bertocci and Huet [6].

The model, although highly simplified, reproduced remarkably well the general behavior of actual systems that underwent a complex corrosion process. The objective of modeling was

to reveal the factors that most influenced surface area dependence of EN in the present system, rather than serve as a fully quantitative predictive tool. However, model advancement could be introduced in various manners to accommodate future improved knowledge on input variables and processes.[18] For example, detailed polarization kinetics rather than a linear approximation could be used for the cathodic reaction. CPE behavior could be directly modeled into the time domain response to both fast anodic and slow cathodic stages instead of assuming simple capacitive behavior.[11-12] As an alternative (already explored in preliminary calculations[20] separate capacitance values could be used for both stages. Randomization of the anodic charge value can also be easily introduced for a more realistic appearance of simulated EN records in the smallest A_S realizations.

The findings on the present systems may be applicable to other EN situations as well[6], but generalization should be viewed with caution in attention to other possible complicating phenomena. For example, if an important contribution to the EN were random metastable crevice corrosion events on the specimen edge, their frequency would be proportional to perimeter length rather to surface area with consequent deviation from the trends observed here. If potential fluctuations were sufficiently large, event interdependence would result through the commonly observed potential dependence on nucleation rate of localized corrosion[10]. Interdependence obtains also if some events involve reactivation of previous event sites or, as observed here, the rate of events becomes time dependent through site exhaustion or a similar mechanism. Custom treatment of these and comparable factors may be needed for specific systems.

CONCLUSIONS

The magnitude of potential electrochemical noise of three aluminum alloys in aerated chloride solutions decreased approximately with increasing square root of specimen surface area in contact with the electrolyte.

The experimental behavior was consistent with the predictions of a simplified model that assumed random generation of similar independent anodic events at a rate proportional only to the specimen area. The anodic potential step from each individual event decreased with increasing specimen area reflecting the corresponding increase in interfacial admittance. This factor, coupled with statistical addition of the contribution of individual events, resulted in a model output reproducing the observed inverse square root dependence on area. The model applicability was demonstrated by nearly replicating experimental behavior when using as input interfacial polarization parameters that were obtained from independent electrochemical impedance and potentiodynamic tests.

REFERENCES

1. D.E. Williams, DECHEMA Monographien., 101 (1986): p. 253.

2. K. Sasaki, P.W. Levy, H.S. Isaacs, Electrochemical and Solid-State Letters, 5, 8 (2002): p. B25.

3. R.A. Cottis, M.A.A Al-Awadhi, H. Al-Mazeedi, S. Turgoose, Electrochim. Acta, 46 (2001): p. 3665.

4. J.W. Isaac, K.R. Hebert, Journal of Electrochemical Society, 146, 2 (1999): p. 502.

5. P.C. Pistorius, Corrosion, 53, 4 (1997): p. 273.

6. U. Bertocci, F. Huet, Corrosion, 51, 2 (1995): p. 131.

7. J.C. Uruchurtu, J.L. Dawson, Corrosion, 43, 1 (1987): p. 19.

8. P.R. Roberge, "Quantifying the Stochastic Behavior of Electrochemical Noise Measurement During the Corrosion of Aluminum", Electrochemical Noise Measurement for Corrosion Applications, ASTM STP 1277, Kearns, J.R., Scully, J.R., Roberge, P.R., Reichert, D.L. & Dawson, J.L., Eds., American Society for Testing and Materials, pp. 142-156 (1996).

9. S.T. Pride, J.R. Scully, J.L. Hudson, "Analysis of Electrochemical Noise from Metastable Pitting in Aluminum, Aged Al-2%Cu, and AA 2024-T3", Electrochemical Noise Measurement for Corrosion Applications, ASTM STP 1277, Kearns, J.R., Scully, J.R., Roberge, P.R., Reichert, D.L. & Dawson, J.L., Eds., American Society for Testing and Materials, pp. 307-331 (1996).

10. S.T. Pride, J.R. Scully, J.L. Hudson, Journal of Electrochemical Society, 141, 11 (1994): p. 3028.

11. A.A. Sagüés, S.C. Kranc, E.I. Moreno, Corrosion Science, 37, (1995): p.1097.

12. A.A. Sagüés, S.C. Kranc, E.I. Moreno, Electrochim. Acta, 41 (1996): p.1239. (see also note by same authors/Journal in Vol 41, p.2661, 1996).

13. M. Urquidi-Macdonald, S. Real, D.D. Macdonald, Electrochim. Acta, 35 (1990): p. 1559.

14. R.A. Cottis, Journal of Corrosion Science and Engineering, 3, Paper 4 (2000).

15. R.A. Cottis, H.A. Al-Mazeedi, S. Turgoose, "Measures for the Identification of Localized Corrosion from Electrochemical Noise Measurements", Corrosion/2002, paper No. 02329 (Houston, TX: NACE International, 2002).

16. S. Paul, P.K. Mitra, S.C. Sirkar, Corrosion, 49 (1993): p.178.

17. P. Roberge, D. Lenard, J. Applied Electrochemistry, 28 (1998): p. 405.

18. U. Bertocci, F. Huet, B. Jaoul, P. Rousseau, Corrosion, 56 (2000): p. 675.

19 N. Arley, K. Rander Buch, "Introduction to the Theory of Probability and Statistics", J. Wiley & Sons Inc, New York (1950).

20. I. Arrieta, M.S. Thesis "The Effect of Surface Area on Electrochemical Noise of Aluminum Alloys 1100, 2024 And 5052 in Chloride Media", University of South Florida, Tampa, Florida 2003.

21. H.P. Goddard, W.B Jepson, M.R. Bothwell, R.L. Kane, "The Corrosion of Light Metals", John Wiley & Sons Inc, New York (1967).

TABLE 1
ALLOY DESIGNATIONS AND COMPOSITION – wt%

Component	1100-H14* (UNS A91100)	2024-T3** (UNS A92024)	5052-H32* (UNS A95052)
Al	99.0	93.0	97.0
Cu	-	4.6	-
Mg	-	1.3	2.5
Si	-	0.1	-
Others	1.0	1.0	0.5

* nominal composition[21]
** reported by manufacturer.

TABLE 2
RESULTS FROM POTENTIODYNAMIC AND IMPEDANCE EXPERIMENTS

Alloy	Specimen	Y_0 ($\mu F.s^n/cm^2$)	N	$ß_c$ @ OCP (V/decade)	ic @ OCP ($\mu A/cm^2$)	Rp @ OCP $k\Omega\ cm^2$
1100	A1	15.7	0.54	-0.48	1.2	170
	A8	12.7	0.64	- 0.55	1.2	190
2024	B1/*B9**	16.5	0.69	*-0.33*	*2.0*	*72*
	B2	13.8	0.63	-0.46	3.7	54
5052	C8	10.4	0.75	-0.25	0.7	150
	C11	10.0	0.78	-0.23	1.0	120

*Results from B9 indicated in italics.

TABLE 3
INPUT AND DERIVED INPUT VARIABLES OF THE EN MODEL

A_s (cm^2)	n_e ($cm^{-2}s^{-1}$)	N_{ev}	C_{eff} ($\mu F/cm^2$)	$q_{ev}.10^8$ (coul)	R_p ($k\Omega.cm^2$)	h_{ev} (mV)	τ (s)
0.04	5	60	20	-2	130	25	2.6
0.2		300				5	
4		6000				.25	

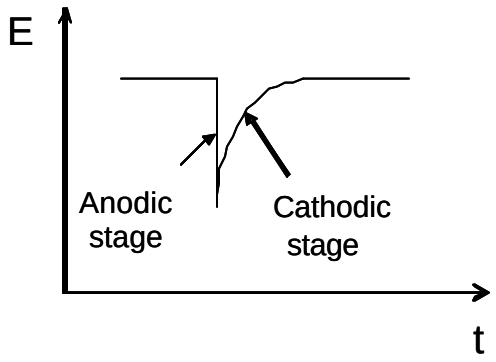

FIGURE 1- Idealized EN event

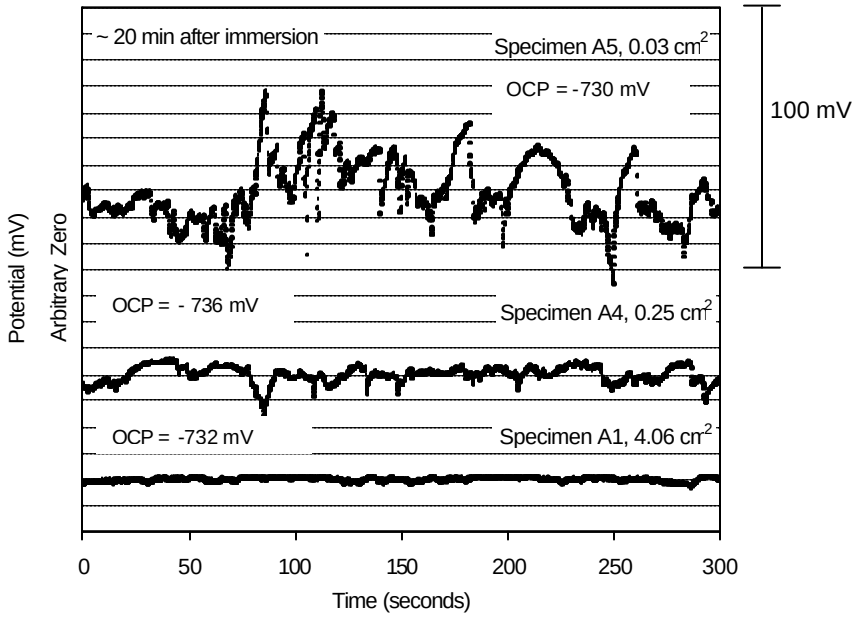

FIGURE 2 - OCP noise for alloy 1100 in 3.5 wt% NaCl ~ 20 min after immersion.

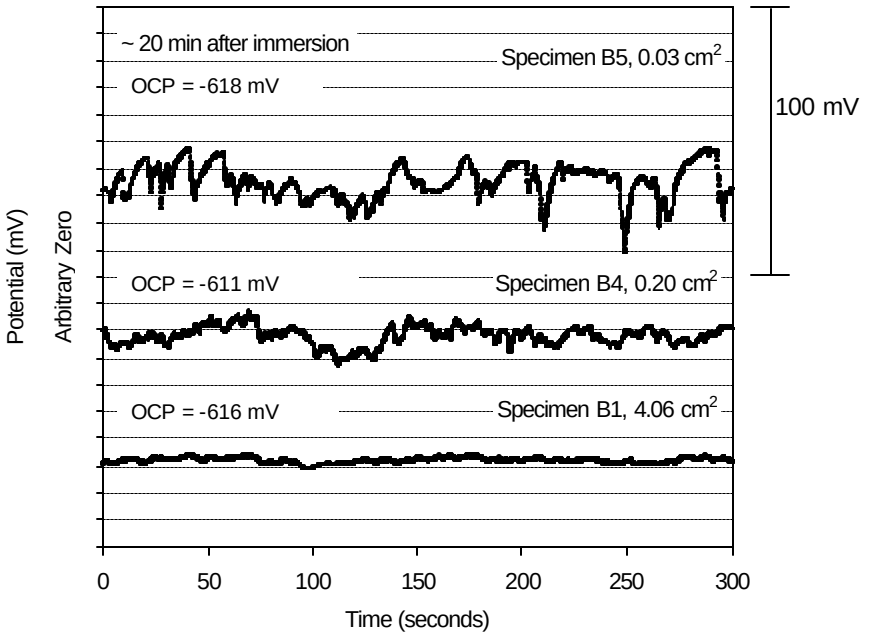

FIGURE 3 - OCP noise for alloy 2024 in 3.5 wt% NaCl ~ 20 min after immersion

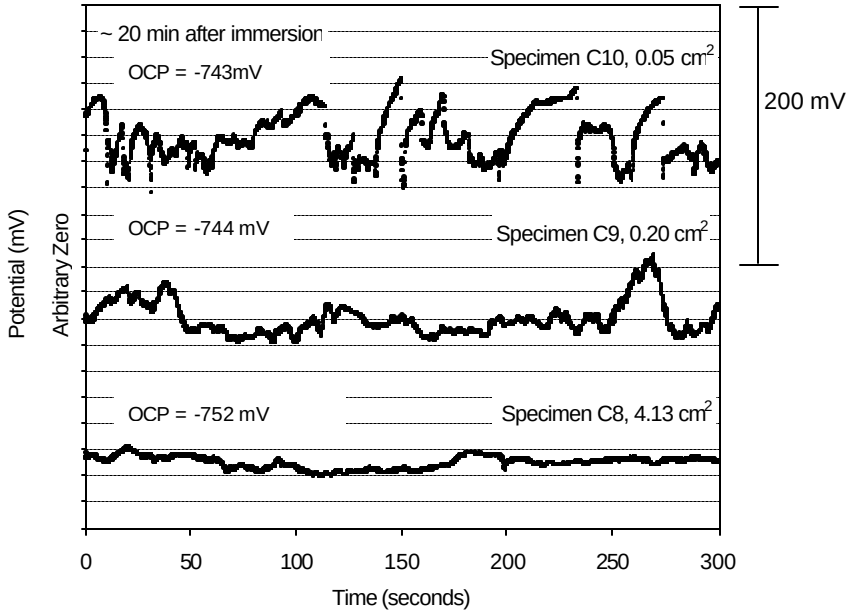

FIGURE 4 - OCP noise for alloy 5052 in 3.5 wt% NaCl ~ 20 min after immersion

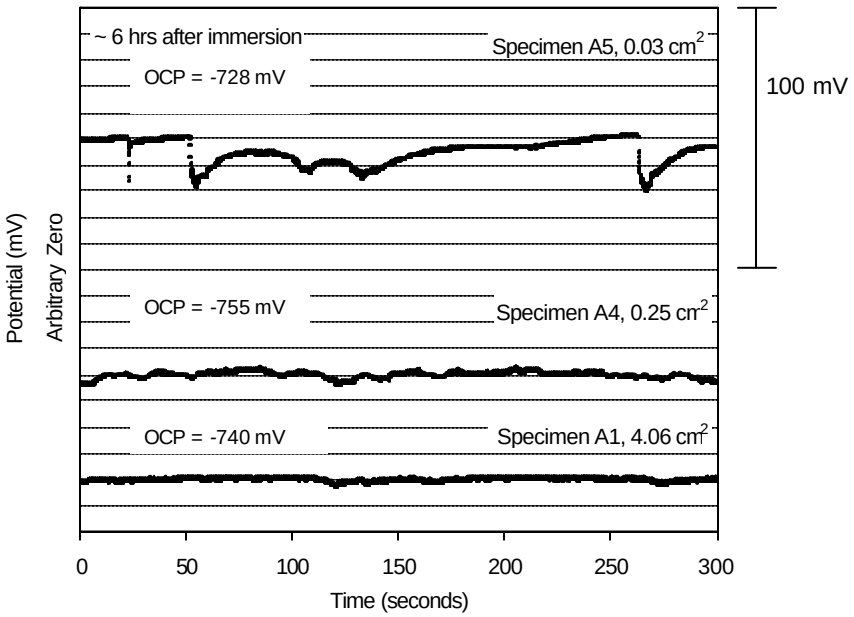

FIGURE 5 - OCP noise for alloy 1100 in 3.5 wt% NaCl ~ 6 hrs after immersion

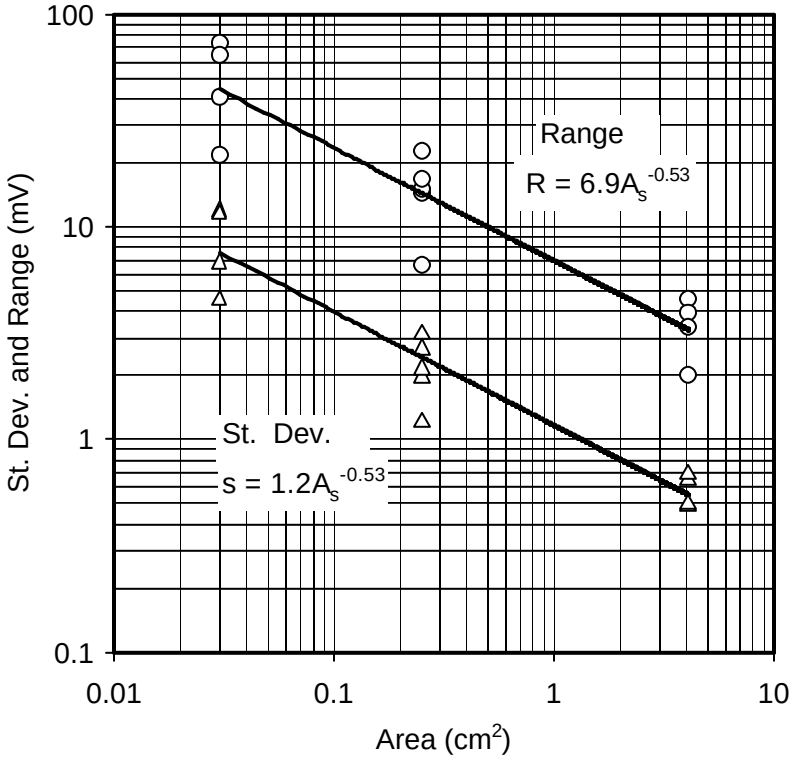

FIGURE 6 - Standard deviation and range for alloy 1100. Signals within the first 6 hours after immersion were considered for this analysis

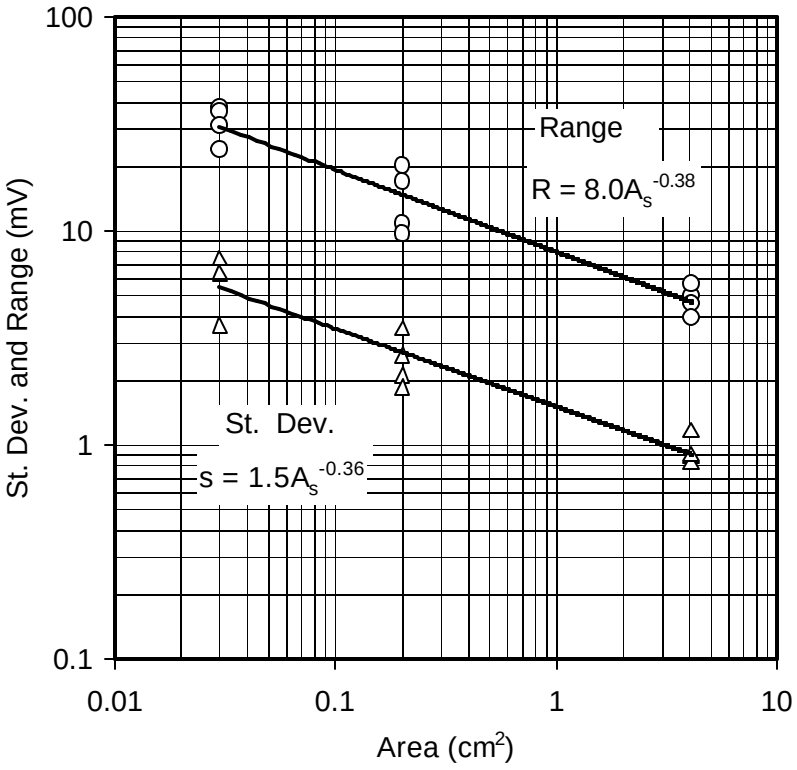

FIGURE 7 - Standard deviation and range for alloy 2024. Signals within the first 3 hours after immersion were considered for this analysis

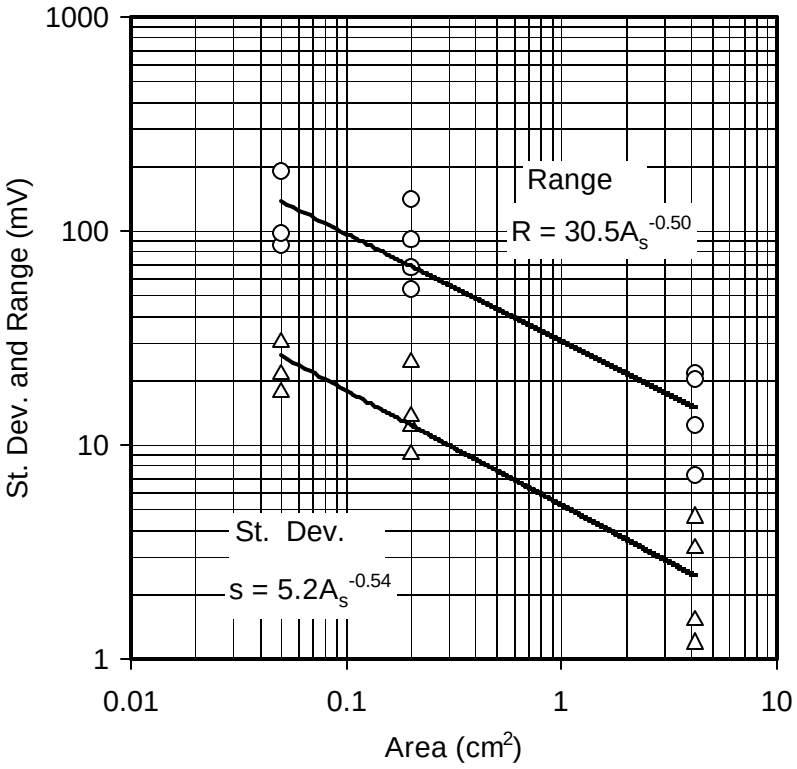

FIGURE 8 - Standard deviation and range for alloy 5052. Signals within the first 6 hours after immersion were considered for this analysis

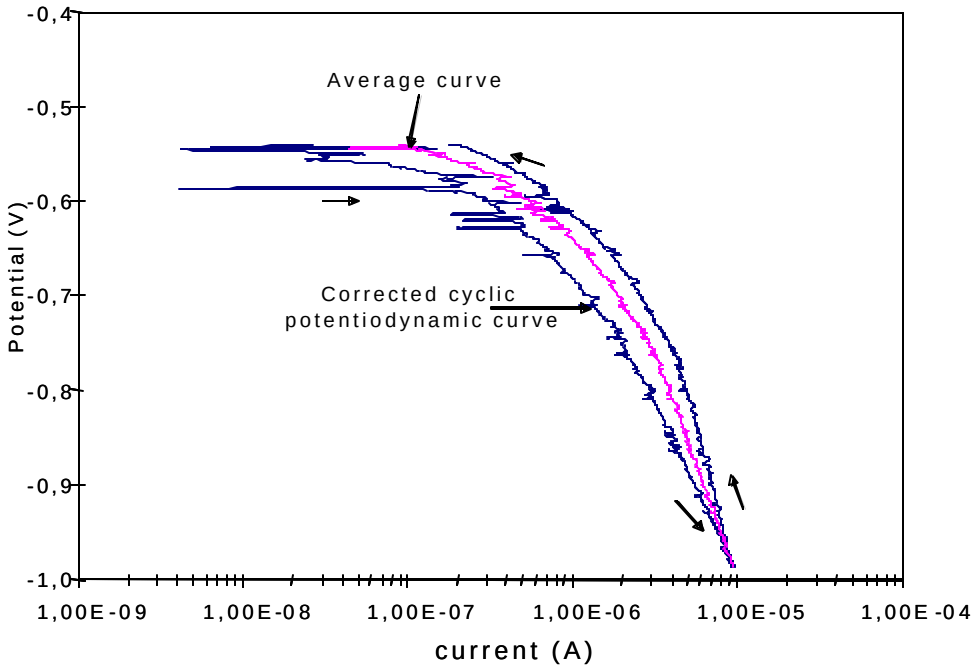

FIGURE 9 - Cyclic potentiodynamic curves for aluminum alloy 5052 in distilled water. Specimen area = 4.13 cm^2 . The displayed data were corrected for solution resistance.

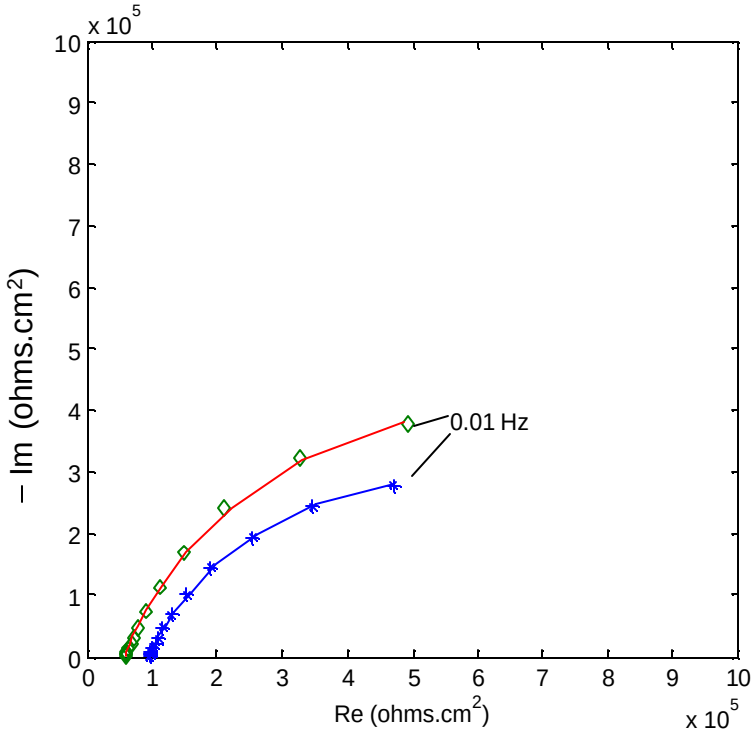

FIGURE 10 – Example of Nyquist EIS response (Duplicate tests of alloy 5052 in distilled water, 4 points per frequency decade).

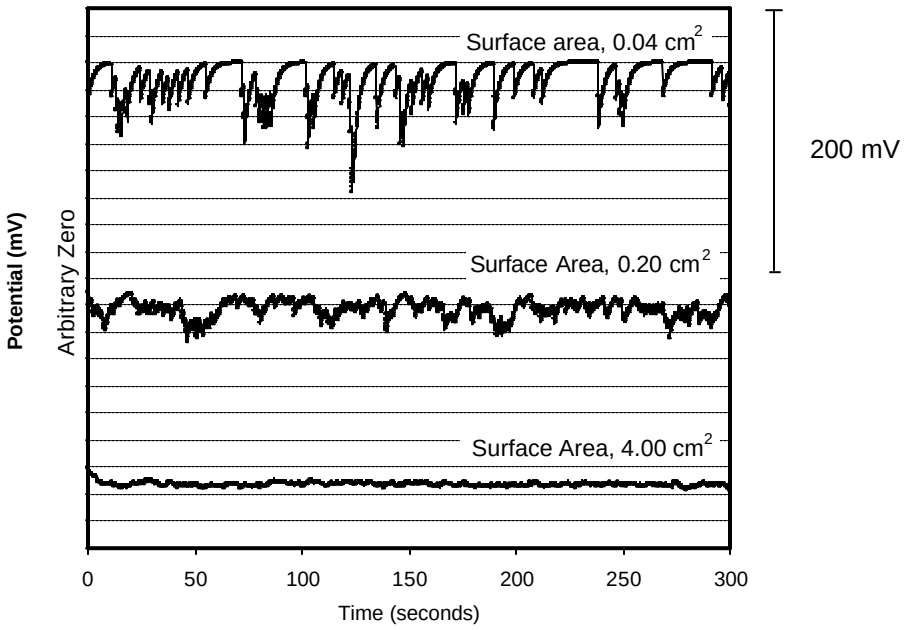

FIGURE 11 – Typical model output EN records.

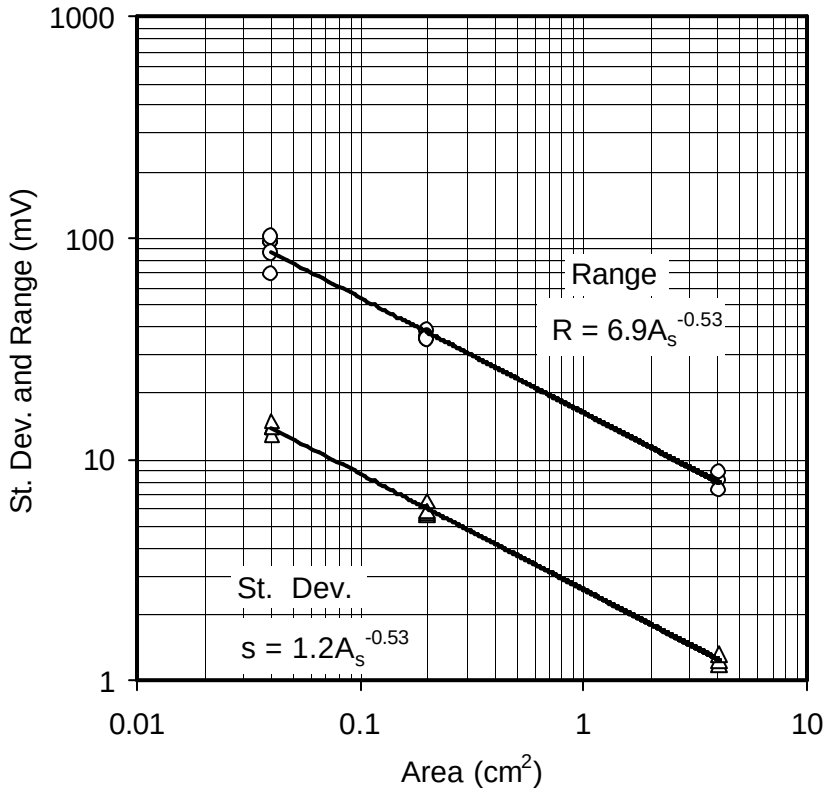

FIGURE 12 - Standard deviation and range of the model output EN records.